Available online at www.sciencedirect.com

ScienceDirect

Procedia Engineering 161 (2016) 833 – 838

Procedia Engineering

www.elsevier.com/locate/procedia

World Multidisciplinary Civil Engineering-Architecture-Urban Planning Symposium 2016, WMCAUS 2016

Bond-slip Modelling of FRP Sheets Externally Bonded to Concrete Beam

Osama Ahmed Mohamed[a,*], Rania Khattab[a]

[a]*College of Engineering, Abu Dhabi University, PO Box 59911, Abu Dhabi, United Arab Emirates*

Abstract

Use of fibre-reinforced polymer (FRP) sheets to strengthen a deficient reinforced concrete structural element has become a popular economic repair and retrofit method. Debonding of FRP sheets from the concrete surface is still a common failure mode that is under investigation. The characteristics of the bond between the externally-bonded FRP sheets and the concrete substrate play a crucial role in the failure process of the strengthened beams. In this paper, a finite element model was implemented using the commercial program ANSYS to examine the stresses and strains along the bond length in the FRP sheets. The peak stresses and strains predicted by the American ACI 440.2R-08 code and Italian CNR- DT 200R1 code were compared with the finite element results.

Peer-review under responsibility of the organizing committee of WMCAUS 2016

Keywords: bonding; Ansys; concrete; FRP; strength.

1. Introduction

To study the mechanism of FRP debonding from the concrete, a reliable bonding model is necessary. Several researchers have proposed various bond models based on experimental studies.

Experimental studies [1,2] showed that the major factors affecting bond-slip between the concrete and the FRP sheets include: concrete compressive strength, f_c'; bond length, L, up to a certain effective bond length, L_e; axial stiffness, $E_p t_p$ of FRP laminate; ratio of width of the FRP plate to the concrete beam b_p/b_c; axial stiffness of the adhesive

* Corresponding author. Tel.: + 971- 2 5015752; fax: +971- 2 5860182.
E-mail address: osama.mohamed@adu.ac.ae

Peer-review under responsibility of the organizing committee of WMCAUS 2016
doi:10.1016/j.proeng.2016.08.723

material, $E_a t_a$; and adhesive compressive strength, f_a. The FRP-to-concrete interface/bond plays a major role in full utilization of the strength and the debonding failure of the FRPs [3].

The shear capacity of FRP sheets is to be evaluated according to two failure modes: FRP debonding and FRP rupture. When FRP sheets are applied to one side of the beam, FRP sheets fail by debonding while in the case of wrapped FRP sheets, rupture failure is dominant. When U-shaped FRP jackets are used to strengthen beams, the shear capacity should be evaluated according to both debonding and rupture of FRP sheets [4, 5]. Double shear test is often used to examine the bond-slip behaviour between FRP and concrete surface and the debonding capacity [6]. Generally, the double shear test is considered more reliable compared to a single shear test.

2. Bond Strength Models

Many models have been proposed for the bond strength between FRP laminates and concrete beam. The model described by Eq. (1) and (2), based on empirical relations calibrated with the experimental data [7].

$$\tau_u = 0.27 . L^{-0.669} \tag{1}$$

$$P_u = \tau_u . L . b_P \tag{2}$$

Where, τ_u is the ultimate shear stress (MPa), L is the bond length (mm), P_u is the bond strength of a joint (N), and b_p is the width of the bonded FRP plate (mm).

According to ACI 440.2R [8], the maximum bond strength is calculated multiplying the maximum strain in the FRP at ultimate state by the elastic modulus of the FRP material, assuming a perfect elastic behaviour. The effective strain in FRP is limited to the strain level at which debonding occurs , ε_{fd} , as defined in Eq. (3). The ultimate strength of the structural member is then found considering the mode of failure for an assumed axial depth as computed in Eqs. (4) to (5).

$$\varepsilon_{fd} = 0.41 \sqrt{\frac{f'_c}{n E_f t_f}} \leq 0.9 \varepsilon_{fu} \tag{3}$$

$$\varepsilon_{fe} = \varepsilon_{cu} \left(\frac{d_f - x}{x} \right) - \varepsilon_{bi} \leq \varepsilon_{fd} \tag{4}$$

$$f_{fe} = \varepsilon_{fe} \cdot E_f \tag{5}$$

$$L_{df} = \sqrt{\frac{n E_f t_f}{\sqrt{f'_c}}} \tag{6}$$

Where, ε_{cu} is the maximum compressive strain in concrete, taken as 0.003, d_f and x are the depth of FRP and the neutral axis, respectively , ε_{fu} is design rupture strain of FRP reinforcement, f_{fe} is the effective stress in the FRP sheets, ε_{fe} is the FRP effective strain , ε_{bi} is the initial substrate strain , E_f is the FRP modulus of elasticity. Bond capacity of FRP is developed over a critical length L_{df} for n FRP layers.

A new version of the Italian guidelines, CNR- DT 200R1 [9] provides a new equation for computing the fracture energy, which has different values depending on the material used, and the effective bond length. The optimal bond length, l_{ed}, is obtained from Eq. (7).

$$l_{ed} = \max\left\{\frac{1}{\gamma_{Rd}\, f_{bd}}\sqrt{\frac{\pi^2 E_f t_f \Gamma_{Fd}}{2}}\,,\quad 200\ mm\right\}\ ;\ f_{bd} = \frac{2.\Gamma_{Fd}}{S_u}\ ;\ \Gamma_{Fd} = \frac{k_b k_G}{FC}\sqrt{f_{cm}\, f_{ctm}} \tag{7}$$

where: E_f and t_f are the modulus of elasticity in the direction of force and the thickness of the FRP, respectively; Γ_{Fd} is the design value of the specific fracture energy; with s_u = 0.25 mm as the design bond strength between FRP and concrete ; γ_{RD} is a corrective factor ; f_{cm} and f_{ctm} are the mean values of the concrete's compressive and tensile strengths, respectively; FC is the confidence factor; k_b is a geometrical corrective factor which is a function of the ratio between the FRP sheet and concrete width.

The maximum design strain value is given by Eq. (8).

$$\varepsilon_{fdd} = \frac{f_{fdd,2}}{E_f} \geq \varepsilon_{sy} - \varepsilon_0\ ;\ f_{fdd,2} = \frac{k_q}{\gamma_{f,d}}\sqrt{\frac{E_f}{t_f}.\frac{2\,k_b k_{G,2}}{FC}\sqrt{f_{cm}\, f_{ctm}}} \tag{8}$$

where, $k_{G,2}$ is a corrective factor calibrated on experimental results and equal to 0.10 mm irrespective of the type of reinforcement, k_q is a coefficient that considers load distributions and is equal to 1.25 for distributed loads and 1.0 for all other load configurations; ε_{sy} is the design yield strain of steel reinforcement ; and ε_0 is the maximum tensile strain present before the FRP is applied.

3. FRP Sheet Debonding Strength Models

FRP sheet or plate debonding has been extensively investigated and various models were developed. In general classified the plate end debonding models into three categories: 1) Shear capacity based models where debonding failure strength is related to the shear strength of concrete only, 2) Concrete tooth models which examines a concrete "tooth" between two adjacent cracked surfaces, 3) Interfacial stress based models in which concrete element adjacent to the end of a bonded plate is subjected to τ, σ_y and σ_x: shear stress, transverse normal stress perpendicular to the adhesive layer and the bonded plate (the peeling stress) and longitudinal stress, respectively [10].

4. Finite Element Analysis Simulation of the Double Shear Test

A finite element analysis model was developed to simulate the double shear test using general purpose software program ANSYS. The purpose was to examine the stress and strain distributions, and to compare the effective bond length approximated using the finite element versus values predicted by two prominent codes. Fig.1 shows the dimensions and details of FRP bonded reinforced concrete prisms that are typically tested. Solid65 element was used to model concrete due to its ability to crush in compression and crack in tension. Cracking is modelled using the smeared crack approach. The reinforcing bars were modelled using LINK180 element while Solid45 element was used to model the FRP sheets. The epoxy that provides bonding/debonding properties is modelled taking into account maximum tensile stress, maximum shear stress, critical fracture energies and separation distance.

The epoxy layer between concrete and FRP was modelled using contact element which employs a contact pair, TARGE170 and CONTA174. TARGE170 was used to represent a 3-D "target" surface and was paired with different contact elements.

4.1. Prediction of effective bond length using two codes.

The following are selected material properties used to determine the effective bond length using ACI 440.2R [9] and CNR-DT 200R1 [9].

$$f'_c = 27.3\,MPa \quad , \quad E_c = 21.0\,MPa \quad , \quad E_f = 165{,}000\ MPa \quad , \quad t_f = 1.3\ mm$$

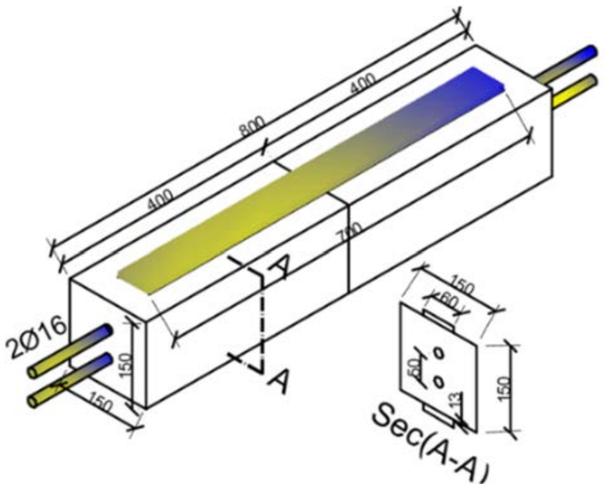

Fig. 1: Dimensions and details of FRP bonded reinforced concrete prisms.

4.1.1. ACI 440.2R Calculation [8]

Effective bond length is given by:

$$L_{df} = \sqrt{\frac{nE_f t_f}{\sqrt{f_c^{'}}}} = \sqrt{\frac{1x165{,}000\ x1.3}{\sqrt{27.3}}} = 202.62\ mm$$

Effective debonding strain is given by:

$$\varepsilon_{fd} = 0.41\sqrt{\frac{f_c^{'}}{nE_f t_f}} = 0.41\sqrt{\frac{27.3}{1x165000\ x1.3}} = 0.0046 \le 0.9\,\varepsilon_{fu}$$

4.1.2. CNR-DT 200R1 Calculation [9]

The specific fracture energy is given by:

$$\Gamma_{Fd} = \frac{k_b k_G}{FC}\sqrt{f_{cm}\, f_{ctm}} = \frac{1.18x\,0.023}{1}\sqrt{27.3x2.73} = 0.2343 \qquad f_{bd} = \frac{2.\Gamma_{Fd}}{S_u} = \frac{2x0.2343}{0.25} = 1.8744$$

The optimal bond length is given by:

$$l_{ed} = \max\left\{\frac{1}{\gamma_{Rd}\, f_{bd}}\sqrt{\frac{\pi^2 E_f t_f \Gamma_{Fd}}{2}} = \frac{1}{1.25x1.8744}\sqrt{\frac{\pi^2 x165000x1.3x0.2343}{2}} = 212.55mm\ ,\ 200\ mm\right\}$$

$$f_{fdd,2} = \frac{k_q}{\gamma_{f,d}}\sqrt{\frac{E_f}{t_f}.\frac{2k_b k_{G,2}}{FC}\sqrt{f_{cm}\, f_{ctm}}} = \frac{1}{1}\sqrt{\frac{165000}{1.3}.\frac{2x1.18x0.1}{1}\sqrt{27.3x2.73}} = 508.52$$

The design strain is given by:

$$\varepsilon_{fdd} = \frac{f_{fdd,2}}{E_f} = \frac{508.52}{165000} = 0.00308 \geq \varepsilon_{sy} - \varepsilon_0$$

In the following section, the finite element method is used to predict the effective bond length as well as the maximum strain. These are compared to the values predicted by the two codes discussed in the previous section of this paper.

5. Results and Discussions

The distribution of elastic strains in the concrete prisms and the FRP sheets is shown in Fig. 2a. It can be seen that the elastic strain distribution at the central point of the prisms and at the very first location of bonded FRP was widely spread and had the highest intensity. Fig. 2b shows contact (bond) stresses at FRP-concrete interface. Due to the symmetry in the double shear test, the contact stresses at the top and bottom of FRP-concrete interfaces are the same. The contact stress value was maximum at the midpoint of the FRP right after the unbonded portion, then started decreasing after this point along the bond length.

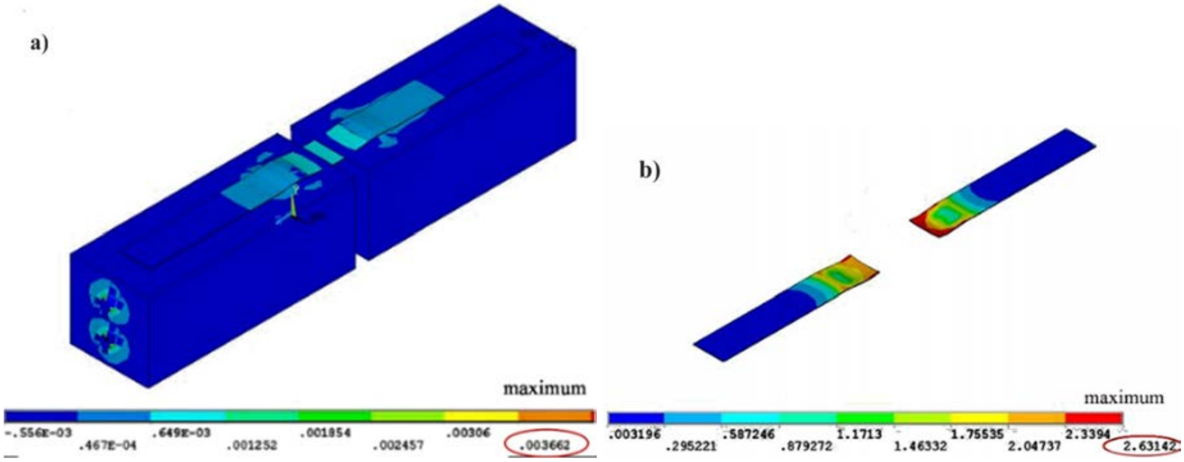

Fig. 2. (a) Elastic strain along bonded area. (b) Contact stress distribution (MPa).

Table 1 shows a comparison between effective bond length and the peak strain determined using the finite element model and the estimated values using ACI 440.2R [8] and CNR-DT 200R1 [9]. Both codes offer more conservative estimates of the effective bond length compared to the finite element model. ACI 440.2R [8] remains conservative in estimating the peak strain while CNR-DT 200R1 [9] provides a much closer to the finite element model.

Table 1. Comparison between effective bond length predicted using finite element model and equation from ACI 440.2R [8] and CNR-DT 200R1 [9] .

	Finite Element Model	ACI 440.2R [8]	CNR-DT 200R1 [9]
Effective bond length	190 mm	202.65 mm	212.55 mm
Maximum strain in FRP	0.00306	0.0046	0.00308

6. Conclusions

In this study, a finite element analysis model of FRP sheets externally bonded to the concrete beam surface was developed using ANSYS software which produced a set of stress and strain distributions along the bond length. The pattern of bond stress along the FRP sheet showed that the maximum shear stress occurred at the first contact point between concrete and FRP sheets, between the two concrete prisms. The strain amplitude in FRP was largest at the first contact point between the two concrete prisms and the intensity of strain diminishes away from the centreline. The two codes ACI 440.2R [8] and CNR-DT 200R1 [9] offer conservative estimates of the effective bond length compared to the finite element model, while only ACI 440.2R [8] was more conservative in estimating the peak strain compared to the finite element model.

Acknowledgements

The authors gratefully acknowledge the financial support of the Center on Sustainable Built Environment at Abu Dhabi University.

References

[1] Lu, X.Z., Teng, J.G., Ye, L.P., Jiang, J.J., Bond-slip models for FRP sheets/plates bonded to concrete. Engineering Structures, Elsevier,2005, 27(6): pp. 920-937.

[2] Yuan, H., Teng, J.G., Seracino, R., Wu, Z.S., Yao, J., Full-range behabiour of FRP-to-concrete bonded joints. Engineering Structures, Elsevier, 2004, 26(5): pp. 553-564.

[3] Obaidat, Y. T., Heyden, S., Dahlblom, O., Evaluation of parameters of bond action between FRP and concrete. Journal of Composites for Construction, 2013, 17(5): pp. 626-635.

[4] Chen, J. F., Teng, J. G.,Shear capacity of FRP-strengthened RC beams: FRP debonding. Construction and Building Materials, 2003a, 17(1): pp. 27–41.

[5] Chen, J. F., Teng, J. G., Shear capacity of FRP-strengthened RC beams: FRP rupture. Journal of Structural Engineering, 2003b, 129(5): pp. 615–625.

[6] Serbescu, A., Guadagnini, M., and Pilakoutas, K., Standardized double-shear test for determining bond of FRP to concrete and corresponding model development. Composites Part B: Engineering, 2013, 55: pp. 277-297.

[7] Hiroyuki, Y., Wu, Z., Analysis of debonding fracture properties of CFS strengthened member subject to tension. In: Non-Metallic (FRP) Reinforcement for Concrete Structures - 3rd International Symposium, Toshiyuki Kanakubo (ed.), Sapporo, Japan, 1997, pp. 287-294.

[8] American Concrete Institute, Guide for the design and construction of externally bonded FRP systems for strengthening of concrete structure - ACI 440.2R-08. Farmington Hill, Mich., USA,2008.

[9] National Research Council of Italy, Guide for the Design and Construction of Externally Bonded FRP Systems for Strengthening Existing Structures - CNR-DT 200R1-2013. Advisory Committee on Technical Regulations for Constructions, Rome,2013.

[10] Teng, J.G., Chen, J.F., Smith, S.T., Lam, L., FRP Strengthened RC Structures. John Willey & Sons, LTD, West Sussex, England, 2002.